

Experience-dependent compartmentalized dendritic plasticity in rat hippocampal CA1 pyramidal neurons

Judit K Makara¹, Attila Losonczy^{1,2}, Quan Wen^{1,2} & Jeffrey C Magee¹

The excitability of individual dendritic branches is a plastic property of neurons. We found that experience in an enriched environment increased propagation of dendritic Na⁺ spikes in a subset of individual dendritic branches in rat hippocampal CA1 pyramidal neurons and that this effect was mainly mediated by localized downregulation of A-type K⁺ channel function. Thus, dendritic plasticity might be used to store recent experience in individual branches of the dendritic arbor.

The arrival of highly correlated input patterns onto individual apical oblique and basal dendrites causes hippocampal CA1 pyramidal cells (CA1PCs) to generate local fast sodium spikes whose propagation strength varies among branches^{1–4}. The propagation strength of dendritic spikes fundamentally determines their effect at the soma, as only strongly propagating spikes evoke precisely timed action potential output². Previously, we reported that spike propagation strength is enhanced by associative pairing of dendritic spikes with backpropagating action potentials or muscarinic acetylcholine receptor activation (branch strength potentiation, BSP²). This raises the possibility that dendritic plasticity participates in hippocampal mnemonic functions by providing a

mechanism for storing complex features encoded in highly correlated input patterns. We hypothesized that experience in a spatially and socially rich environment^{5–7} could induce compartmentalized changes in spike propagation strength in CA1PC dendrites. To test this, we compared spike propagation in perisomatic dendrites of CA1PCs in acute slices prepared from rats that were exposed to an enriched environment for 2–7 d (**Supplementary Methods and Supplementary Fig. 1**) with that of control rats. Experiments were conducted in accordance with institutional regulations (Janelia Farm Institutional Animal Care and Use Committee).

Most perisomatic dendrites form families consisting of primary parent dendrites, terminal daughter dendrites and occasionally intermediate segment(s). The strength of local spike propagation is hierarchically distributed in dendritic families². Primary parent dendrites usually express strong spikes (rate of rise, $dV/dt > 2 \text{ V s}^{-1}$, see ref. 2 and **Supplementary Methods**), whereas propagation in most subordinate branches is weak ($dV/dt < 2 \text{ V s}^{-1}$), with a subgroup of daughter dendrites in which propagation is strong enough to spread into the parent dendrite and evoke its strong spike² (see below). We first systematically measured the propagation strength of dendritic spikes in every possible branch of perisomatic apical oblique dendritic

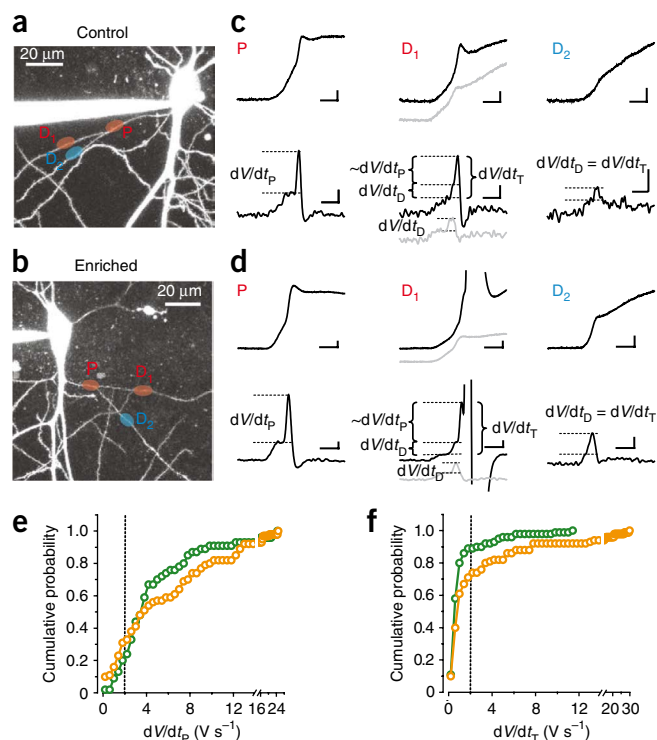


Figure 1 Hierarchical distribution of propagation strength of dendritic spikes in CA1 pyramidal cells of control and enriched rats. **(a,b)** Cells loaded with Alexa488 from control **(a)** and enriched **(b)** rats. Ovals indicate input sites on a primary parent dendrite (P) and the connected terminal daughter dendrites (D₁ and D₂). **(c,d)** V_m (upper) and dV/dt (lower) traces evoked at the input sites in **a** and **b**, respectively. In both cells, input onto P evoked a strong spike with a single dV/dt component (dV/dt_P). Input onto D₁ evoked a strong compound spike (dV/dt_T) with two components, dV/dt_D (D₁'s own spike) and dV/dt_P (the spike propagated into P). dV/dt_D could be resolved (gray traces, shifted for clarity) at more distal input sites **(c)** or by hyperpolarization **(d)**. Input onto D₂ evoked a weak spike that did not propagate into the parent branch ($dV/dt_D = dV/dt_P$). Scale bars represent 1 mV (V_m traces) or 1 V s⁻¹ (dV/dt traces), 2 ms. **(e,f)** Cumulative probability of primary parent dendrites **(e)**, dV/dt_P and of the total spike of terminal daughter dendrites **(f)**, dV/dt_T in control **(green)** and enriched **(yellow)** cells. Dashed line indicates 2 V s⁻¹. Error bars represent s.e.m.

¹Howard Hughes Medical Institute, Janelia Farm Research Campus, Ashburn, Virginia, USA. ²Present address: Department of Neuroscience, Columbia University, New York, New York, USA (A.L.), Department of Physics, Harvard University, Cambridge, Massachusetts, USA (Q.W.). Correspondence should be addressed to J.K.M. (makaraj@janelia.hhmi.org) or J.C.M. (mageej@janelia.hhmi.org).

Received 28 May; accepted 18 September; published online 8 November 2009; corrected online 17 November 2009 (details online); doi:10.1038/nn.2428

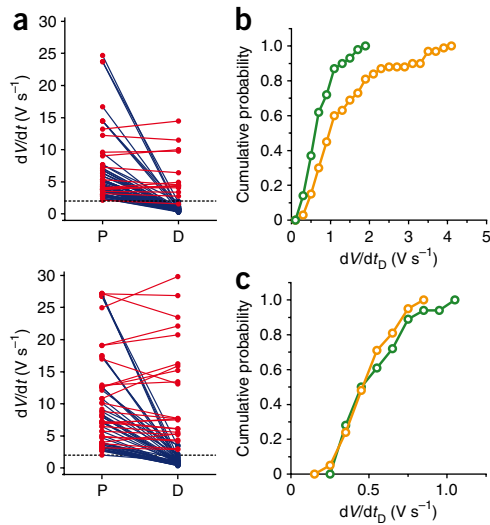


Figure 2 Coupling and dV/dt_D in strong and weak dendritic families. (a) Spike dV/dt of strong parent dendrites (P, dV/dt_P) and of connected daughter dendrites (D, dV/dt_D) in control (upper) and enriched (lower) cells. Red lines indicate coupled P-D pairs, and blue lines indicate noncoupled P-D pairs. Dashed line indicates 2 V s^{-1} . (b) Cumulative probability of dV/dt_D in all terminal daughter branches of strong parent dendrites in control (green) and enriched (yellow) cells. (c) Data are presented as in b, but for terminal branches connected to weak parent dendrites.

families by evoking local Na^+ spikes with two-photon uncaging of MNI-glutamate and measuring spike dV/dt at the soma (Fig. 1a–d).

The spike strength of primary parent dendrites had a similar distribution in control rats as has been previously reported². The majority (79.6%) of primary branches expressed strong spikes, 18.5% had weak spikes and no spike could be evoked in 1.9% (total $n = 54$). In cells from enriched rats, the proportion of strong primary parent branches was 68.9%, whereas 21.3% had weak spikes and no spikes could be evoked in 9.8% (total $n = 61$; Fig. 1e). Thus, the proportion of weak or nonspiking primary branches (resulting in ‘weak’ dendritic families) showed a tendency to increase in enriched rats (control, 11 of 54; enriched, 19 of 61; $P = 0.189$), but most primary dendrites still expressed strong spikes (‘strong’ dendritic families). Although weak primary parent dendrites had similar propagation strength in the two groups (control, $1.40 \pm 0.18 \text{ V s}^{-1}$, $n = 10$; enriched, $1.39 \pm 0.11 \text{ V s}^{-1}$, $n = 13$; $P = 0.95$), dV/dt_P of strong primary parent branches was slightly larger in enriched cells (control, $6.12 \pm 0.76 \text{ V s}^{-1}$, $n = 43$; enriched, $8.21 \pm 0.82 \text{ V s}^{-1}$, $n = 42$; $P = 0.026$).

Next, we analyzed the distribution of spike strength evoked in terminal daughter branches, tested at $15\text{--}40 \mu\text{m}$ from the branch point. The total spike strength (dV/dt_T ; definitions in Fig. 1a–d and Supplementary Methods) was markedly different between control and enriched terminal branches (Fig. 1f), as terminal dendrites with strong spikes were much more frequent in enriched cells (24 of 84, 28.6%) than in control cells (9 of 83, 10.8%; $P = 0.004$).

To further understand this, we separately looked at the spike strength in terminal branches connected to strong versus weak parent dendrites (Fig. 2). The effect of a terminal branch spike at the soma is in part determined by the strength of the primary branch to which it is connected. If the primary branch is strong, the strength of the terminal branch is determined by whether the local terminal

branch spike can overcome the impedance load of the branch point and recruit the strong spike of the parent dendrite (coupled branches) or not (noncoupled branches)². Accordingly, in coupled terminal daughter branches connected to strong parent dendrites, the total spike (dV/dt_T) has two components, the first related to the spike of the daughter branch itself (dV/dt_D) and the second of similar size as the spike of the parent dendrite ($\sim dV/dt_P$; see Fig. 1c,d)². Coupling can be expressed by the spike ratio, calculated as the ratio of dV/dt_T to dV/dt_P . The spike ratio had a bimodal distribution in both control and enriched cells, with noncoupled branches having spike ratios on average ~ 0.16 and coupled branches with spike ratios of ~ 1 (Fig. 2a and Supplementary Fig. 2). However, comparing the frequency of terminal daughter branches that were coupled to strong parent dendrites, we found that coupling probability was twofold higher in enriched cells (23 of 67 branches, 34.3%) than in control cells (14 of 86 branches, 16.3%; $P = 0.0097$; Fig. 2a).

The higher probability of coupled daughter-parent dendrites in enriched cells may result from stronger spike propagation in the daughter segment. Indeed, dV/dt_D in terminal daughter branches of strong parent dendrites was increased compared with control (control: $0.79 \pm 0.04 \text{ V s}^{-1}$, median of 0.73 V s^{-1} , $n = 86$; enriched: $1.42 \pm 0.12 \text{ V s}^{-1}$, median of 1.10 V s^{-1} , $n = 67$; $P < 0.001$; Fig. 2b). In fact, in some enriched terminal branches (13 of 67, 19.4%), dV/dt_D was larger than 2 V s^{-1} , a value that was rarely observed in control cells. The effect on dV/dt_D could not be explained by a difference in the distance of the input site along oblique dendrites (Supplementary Fig. 3), and the alterations in branch excitability were uniformly observed in a large fraction of the enriched cell population as opposed to large changes

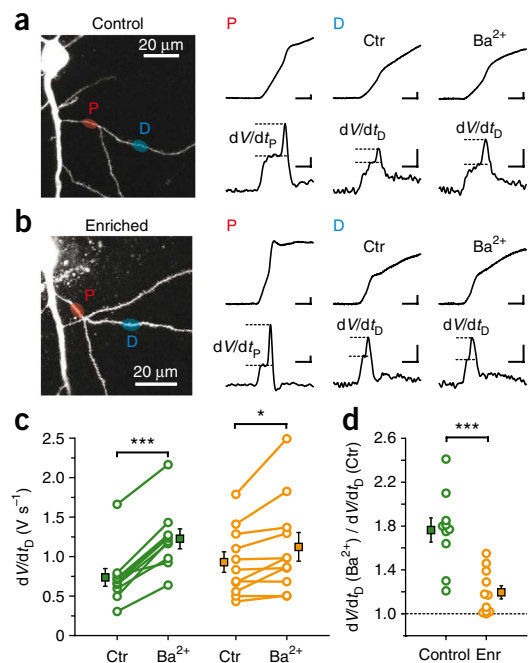


Figure 3 A-type K^+ channel function is reduced by enrichment in terminal daughter dendrites of strong dendritic families. (a,b) Left, image stacks of cells loaded with Alexa488 from control (a) and enriched (b) rats. Ovals indicate input sites on a primary parent dendrite (P) and connected terminal daughter dendrite (D). Right, V_m (upper) and dV/dt (lower) traces evoked from parent (P) and daughter (D) before (Ctr) and during (Ba^{2+}) bath application of $200 \mu\text{M}$ Ba^{2+} . Scale bars represent 1 mV (V_m traces) or 1 V s^{-1} (dV/dt traces), 2 ms . (c,d) Summary of the effects of Ba^{2+} on dV/dt_D (c, individual values before (Ctr) and during Ba^{2+} ; d, change in Ba^{2+} relative to Ctr) in control (green) and enriched (yellow) cells. Error bars represent s.e.m.

in only a small fraction (**Supplementary Fig. 4**). Notably, we found a substantial correlation between dV/dt_p and dV/dt_D in enriched, but not in control cells (**Supplementary Fig. 2**). Thus, enrichment forms dendritic families that are composed of both very strong parent and daughter dendrites. Notably, these changes did not result from a general increase of dendritic excitability, as dV/dt_D was not altered in daughter branches of weakly spiking parent dendrites (control, $0.56 \pm 0.05 \text{ V s}^{-1}$, $n = 18$; enriched, $0.52 \pm 0.03 \text{ V s}^{-1}$, $n = 21$; $P = 0.735$; **Fig. 2c**), and the number of strongly spiking parent dendrites and the spike strength in weak parent dendrites (see above) did not increase in enriched cells.

The enhancement of terminal branch spike strength in strong dendritic families closely resembled that observed during BSP². The underlying mechanism of BSP is a downregulation of A-type K⁺ currents² that are sensitive to low concentrations of Ba²⁺ (refs. 2,8). Therefore, we examined the effect of 200 μM Ba²⁺ on comparable weak terminal branches of strong dendritic families in control and enriched cells (**Fig. 3**). Ba²⁺ reliably increased dV/dt_D in control cells (from $0.74 \pm 0.11 \text{ V s}^{-1}$ to $1.23 \pm 0.13 \text{ V s}^{-1}$, $176 \pm 11\%$, $n = 10$, $P < 0.001$; **Fig. 3a,c,d**), but had a much weaker effect in enriched cells (from $0.93 \pm 0.13 \text{ V s}^{-1}$ to $1.12 \pm 0.18 \text{ V s}^{-1}$, $120 \pm 6\%$, $n = 11$, $P = 0.019$; **Fig. 3b–d**; main effect, $P = 0.003$, repeated measures ANOVA). This indicates that downregulation of A-type K⁺ currents is important for the effect of enrichment on terminal branch spike strength, similar to BSP *in vitro*.

Because dendritic geometry may affect spike propagation^{9,10}, we tested whether the morphology of the studied dendrites was changed by our short enrichment exposure. Digital reconstruction of perisomatic apical dendritic arbors of Alexa488-filled CA1PCs¹¹ from slices of control ($n = 10$) and enriched ($n = 10$) rats did not reveal any differences in arbor radius, total dendritic length, number of branch points and Sholl analysis (**Supplementary Fig. 5**).

In summary, exposure to an enriched environment leads to compartmentalized changes in the distribution of dendritic spike propagation in CA1PCs, indicating that the electrical properties of individual dendritic branches can be modified by *in vivo* experience. The increase of excitability in specific branches is mediated primarily by decreases in the activity of Ba²⁺-sensitive voltage-gated

K⁺ channels (probably Kv4.2, ref. 2). Thus, recent experience induces plasticity of dendritic branch excitability that shares many features with the previously reported *in vitro* associative plasticity referred to as BSP. Therefore, we would infer that the enrichment-induced alterations reflect an *in vivo* BSP-like storage process that takes place during the learning of a complex environment, triggered by the repeated occurrence of highly correlated input patterns arriving during awake and sleep sharp waves^{12–14}. Nevertheless, contribution of other factors, such as physical activity or altered stress levels, cannot be ruled out. Future experiments modifying hippocampal activity patterns and BSP induction/expression during experience should help to understand the role of compartmentalized regulation of dendritic excitability in hippocampal information storage.

Note: Supplementary information is available on the Nature Neuroscience website.

AUTHOR CONTRIBUTIONS

J.K.M. and J.C.M. designed the study. J.K.M. and A.L. conducted the electrophysiological recordings. J.K.M. analyzed most of the electrophysiological data. Q.W. performed and analyzed cell reconstructions. J.K.M. and J.C.M. wrote the paper.

Published online at <http://www.nature.com/natureneuroscience/>.

Reprints and permissions information is available online at <http://www.nature.com/reprintsandpermissions/>.

1. Losonczy, A. & Magee, J.C. *Neuron* **50**, 291–307 (2006).
2. Losonczy, A., Makara, J.K. & Magee, J.C. *Nature* **452**, 436–441 (2008).
3. Golding, N.L. & Spruston, N. *Neuron* **21**, 1189–1200 (1998).
4. Ariav, G., Polsky, A. & Schiller, J. *J. Neurosci.* **23**, 7750–7758 (2003).
5. Rampon, C. & Tsien, R. *Hippocampus* **10**, 605–609 (2000).
6. van Praag, H., Kempermann, G. & Gage, F.H. *Nat. Rev. Neurosci.* **1**, 191–198 (2000).
7. Nithianantharajah, J. & Hannan, A.J. *Nat. Rev. Neurosci.* **7**, 697–709 (2006).
8. Gasparini, S., Losonczy, A., Chen, X., Johnston, D. & Magee, J.C. *J. Physiol. (Lond.)* **580**, 787–800 (2007).
9. Vetter, P., Roth, A. & Häusser, M. *J. Neurophysiol.* **85**, 926–937 (2001).
10. Migliore, M., Ferrante, M. & Ascoli, G.A. *J. Neurophysiol.* **94**, 4145–4155 (2005).
11. Wen, Q., Stepanyants, A., Elston, G.N., Grosberg, A.Y. & Chklovskii, D.B. *Proc. Natl. Acad. Sci. USA* **106**, 12536–12541 (2009).
12. O'Neill, J., Senior, T. & Csicsvári, J. *Neuron* **49**, 143–155 (2006).
13. Wilson, M.A. & McNaughton, B.L. *Science* **265**, 676–679 (1994).
14. Nádasdy, Z., Hirase, H., Czurkó, A., Csicsvári, J. & Buzsáki, G. *J. Neurosci.* **19**, 9497–9507 (1999).